

Supporting information

In-situ Polymerized Electrolyte Layer via Frustrated Lewis Pairs Enables Aqueous Zn Metal Batteries with Ultrahigh Accumulated Capacity of 12 Ah cm⁻²

Yutong Xia^{a1}, Gege Wang^{a,b1}, Jing Wu^{a,b}, Xiaowei Chi^{a}, Yu Liu^{a*}*

^aShanghai Institute of Ceramics, Chinese Academy of Sciences

Shanghai 200050, China

Email: xwchi@mail.sic.ac.cn

Email: yuliu@mail.sic.ac.cn

^bUniversity of Chinese Academy of Sciences

Beijing 100049, China

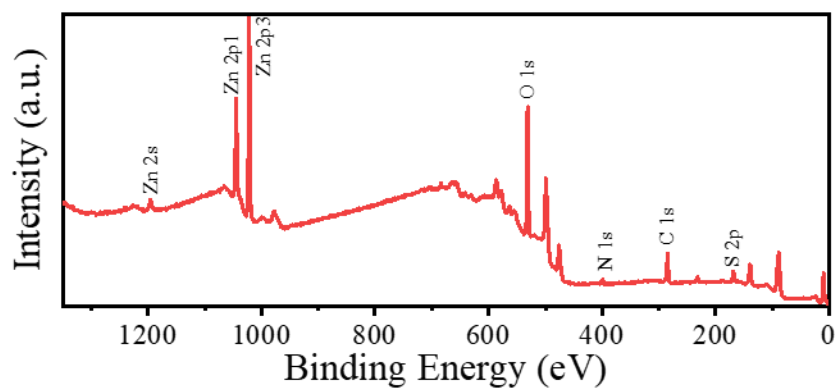


Figure S1. X-ray photoelectron spectroscopy of zinc anode after 36 h of cycling in the electrolyte containing AMPS

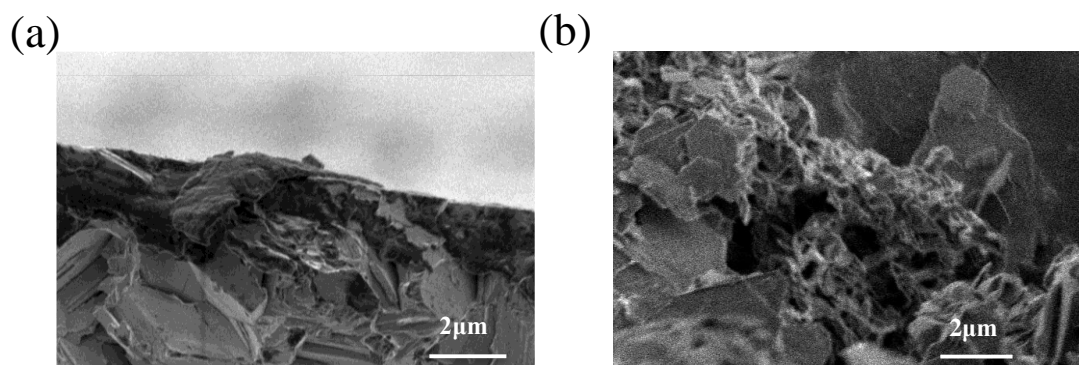


Figure S2. (a)~(b) Cross-sectional and surface SEM images of the interface of electrolyte/Zn anode in the electrolyte without AMPS.

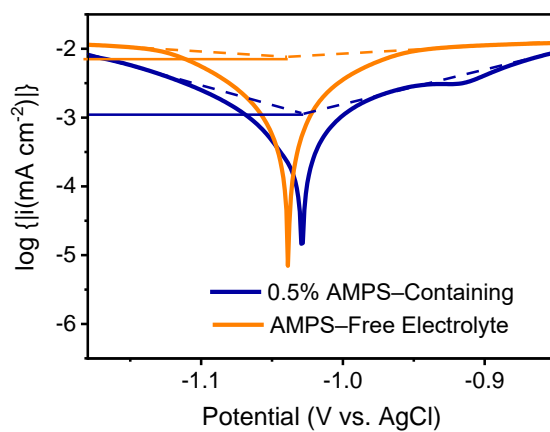


Figure S3. Tafel curves of the Zn metal electrode in the 0.5% AMPS-contained and AMPS-free electrolyte.

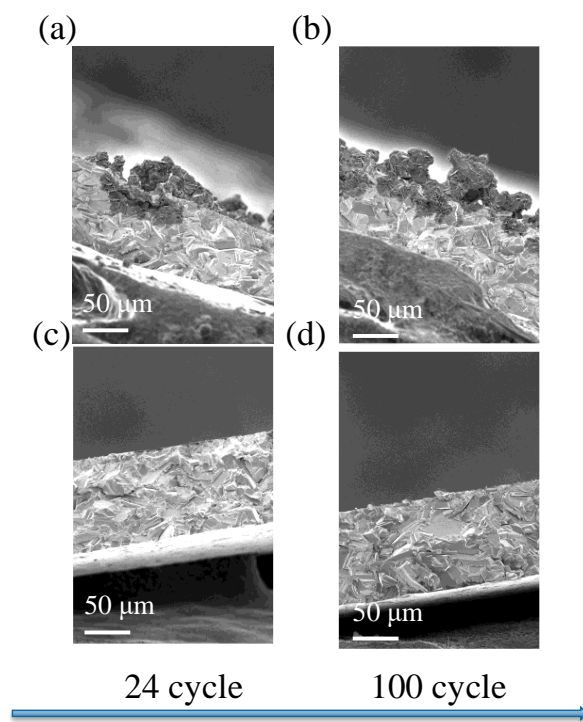


Figure S4. Cross-sectional SEM images of the interface of electrolyte/Zn anode in the electrolyte (a)~(b) without and (c)~(d) with AMPS.

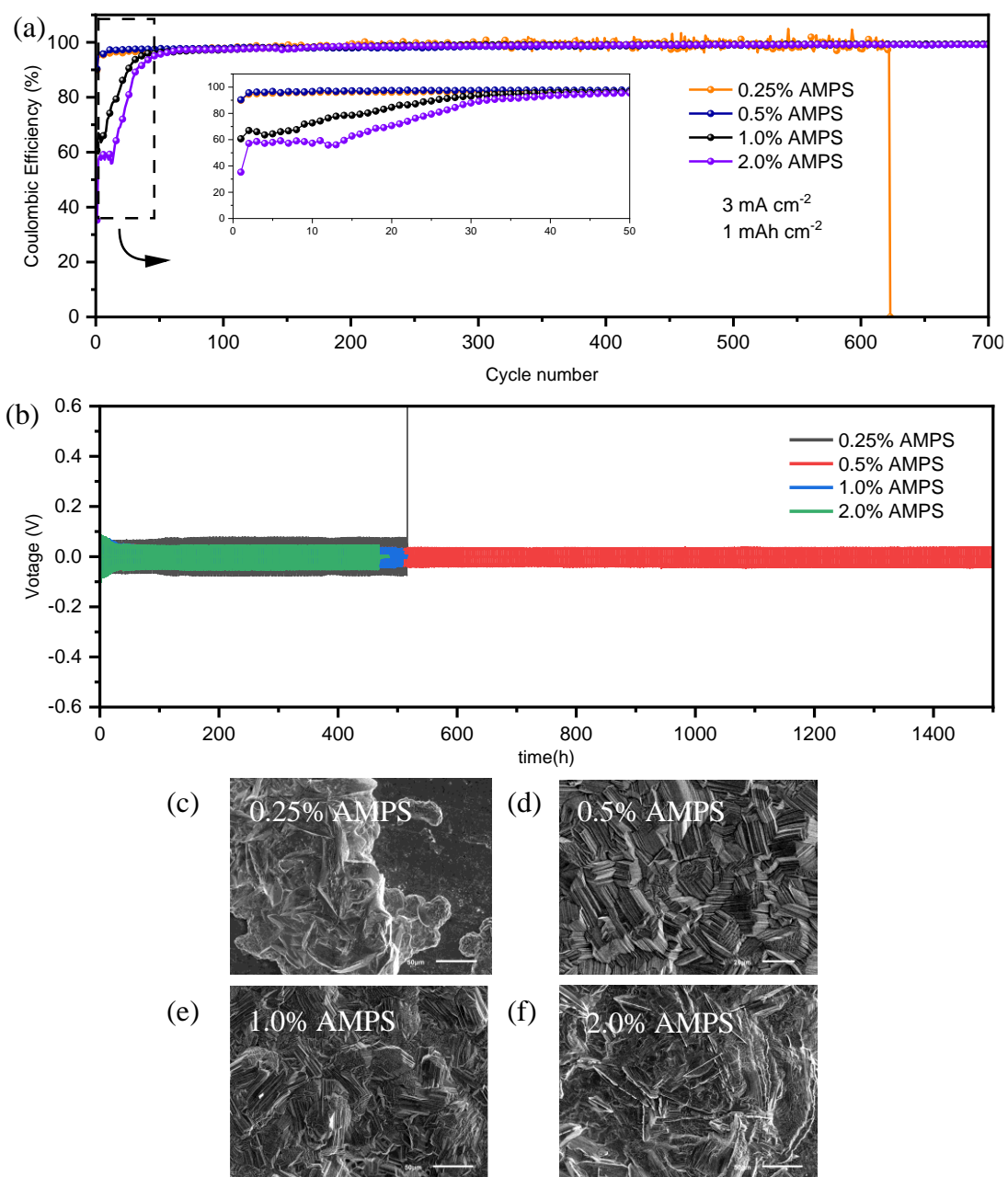


Figure S5. Electrochemical plating/stripping behavior of Zn metal electrode in different concentrations of AMPS in 2m ZnSO_4 electrolyte. a) Coulombic efficiency of Zn||Cu asymmetry cell at a current density of 3 mA cm^{-2} with a fixed capacity of 1 mAh cm^{-2} . b) Voltage profiles of Zn||Zn symmetry cell at a current density of 5 mA cm^{-2} with a fixed capacity of 5 mA h cm^{-2} . c–f) SEM images of the Zn deposits at a current density of 5 mA cm^{-2} with a capacity of 25 mAh cm^{-2} .

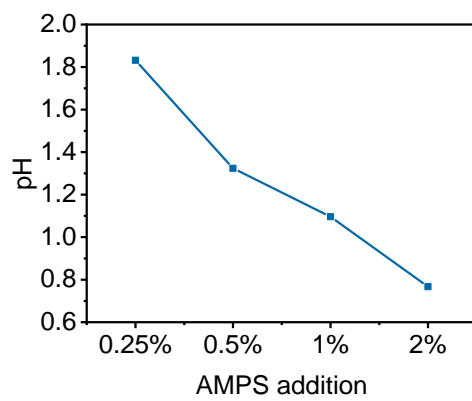


Figure S6. Trend of pH change after addition of 0.25%, 5%, 1% and 2% AMPS to 2M aqueous zinc sulfate solution

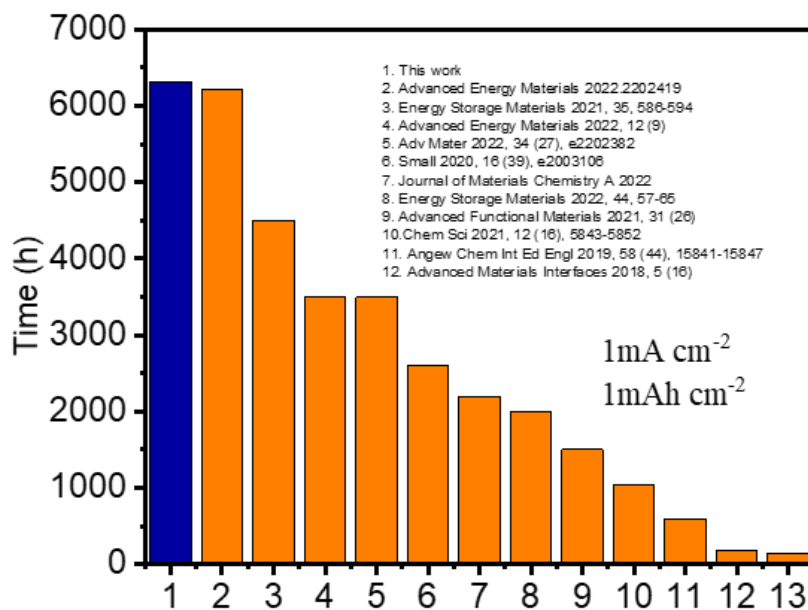


Figure S7. Comparison of the cycling lifespan of the reported Zn||Zn symmetrical cells and this work at 1 mA cm⁻² and 1 mAh cm⁻².

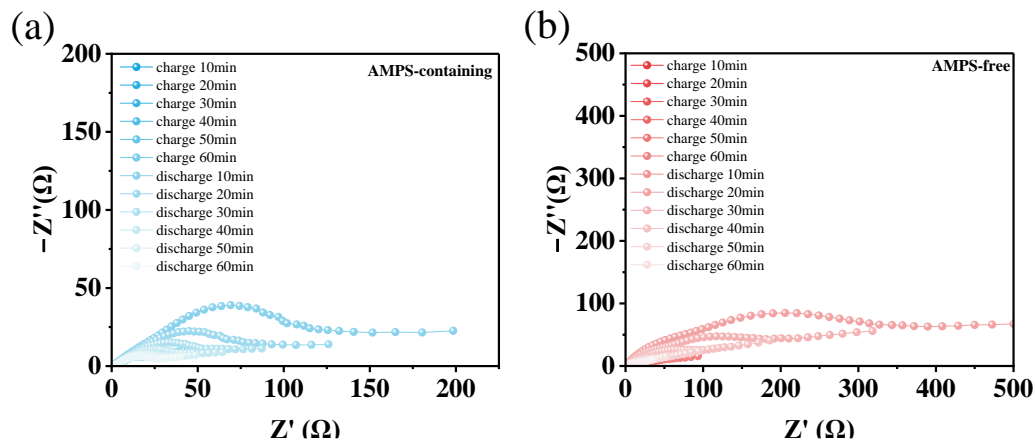


Figure S8. In-situ EIS of Zn||Zn cell using (a) AMPS-Containing and (b) AMPS-Free electrolytes.

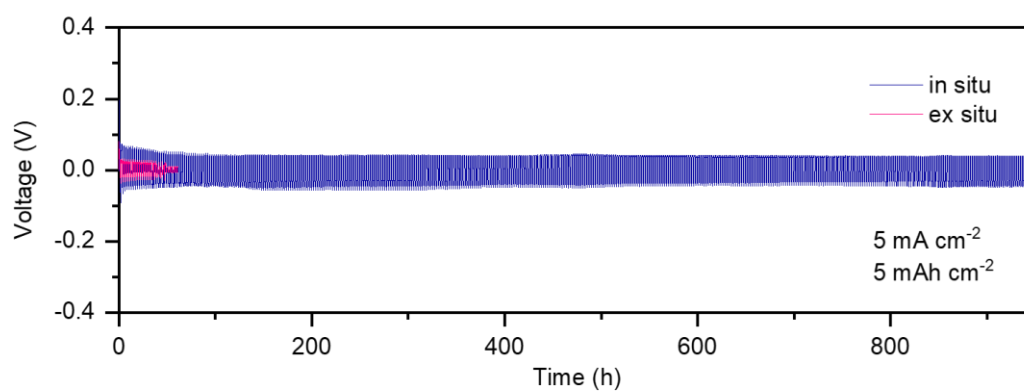


Figure S9. Long-term galvanostatic cycling of Zn||Zn symmetric cells at a current density 5 mA cm^{-2} and capacity of 5 mA h cm^{-2} , with AMPS contained in situ and ex situ.

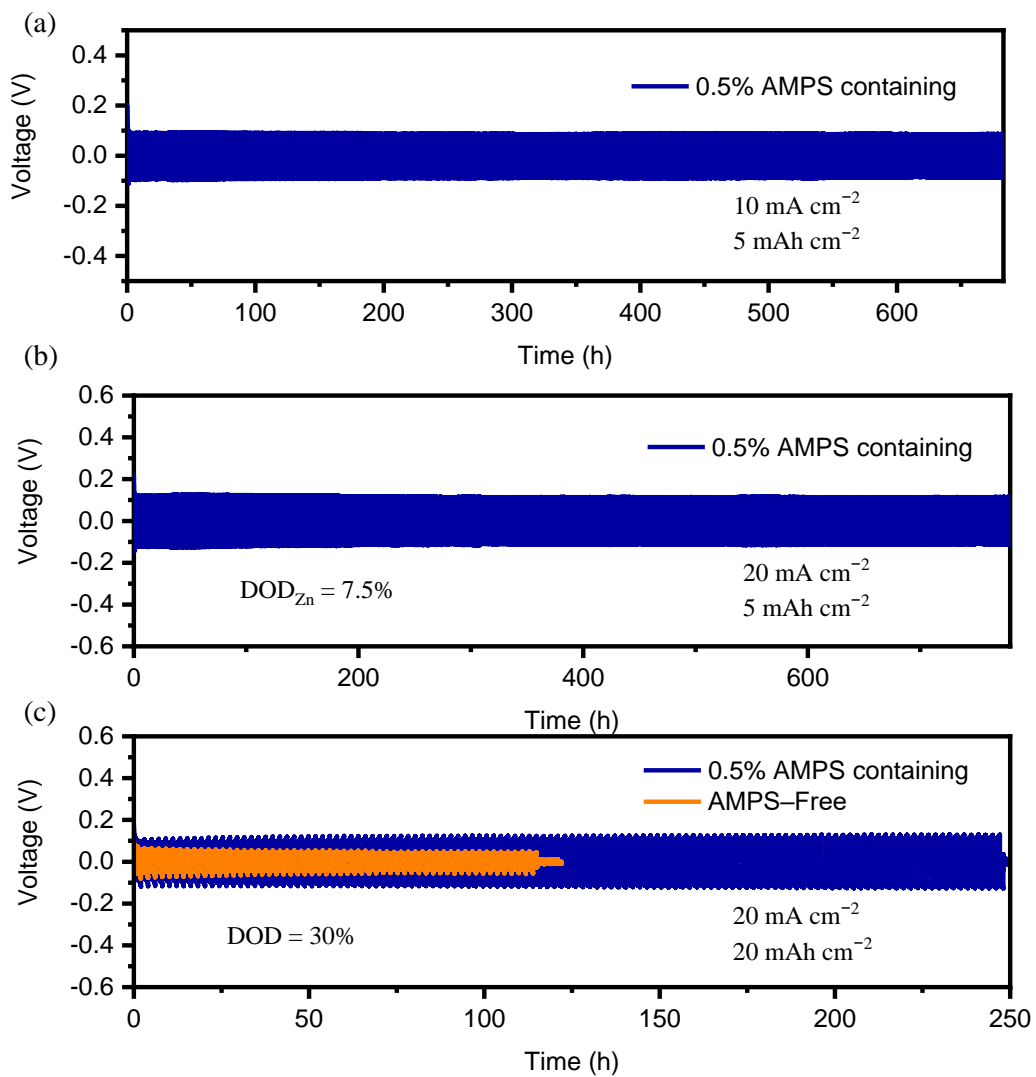


Figure S10. Voltage profiles of Zn||Zn symmetric cells in AMPS-containing and AMPS-free electrolytes cycled at a) 10 mA cm^{-2} and 5 mAh cm^{-2} ; b) 20 mA cm^{-2} and 5 mAh cm^{-2} ($\text{DoD}_{\text{Zn}} = 7.5\%$); c) 20 mA cm^{-2} and 20 mAh cm^{-2} ($\text{DoD}_{\text{Zn}} = 30\%$).

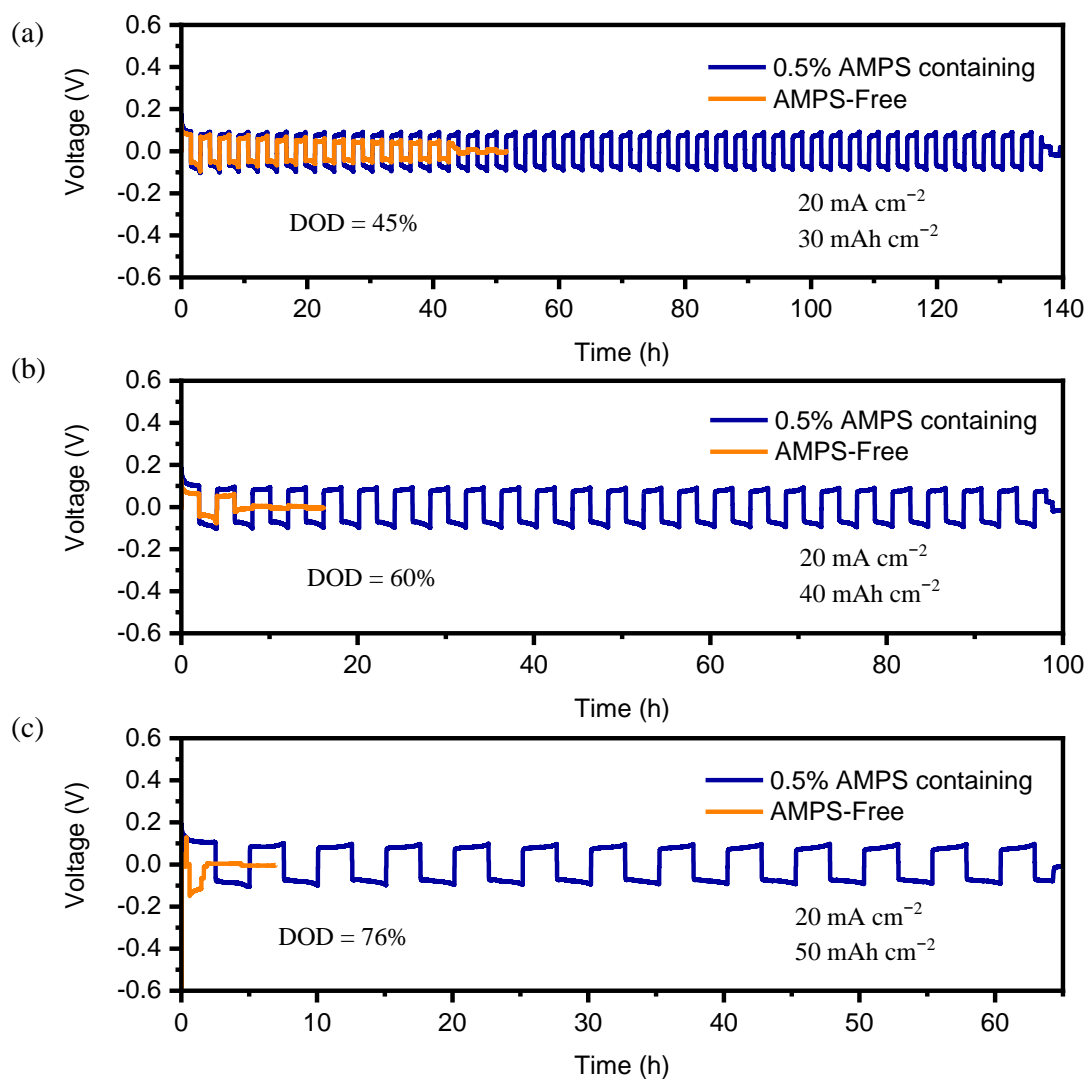


Figure S11. Voltage profiles of Zn||Zn symmetric cells in AMPS-containing and AMPS-free electrolytes cycled at a) 20 mA cm^{-2} and 30 mAh cm^{-2} ($\text{DoD}_{\text{Zn}} = 45\%$); b) 20 mA cm^{-2} and 40 mA h cm^{-2} ($\text{DoD}_{\text{Zn}} = 60\%$); c) 20 mA cm^{-2} and 50 mA h cm^{-2} ($\text{DoD}_{\text{Zn}} = 75\%$).

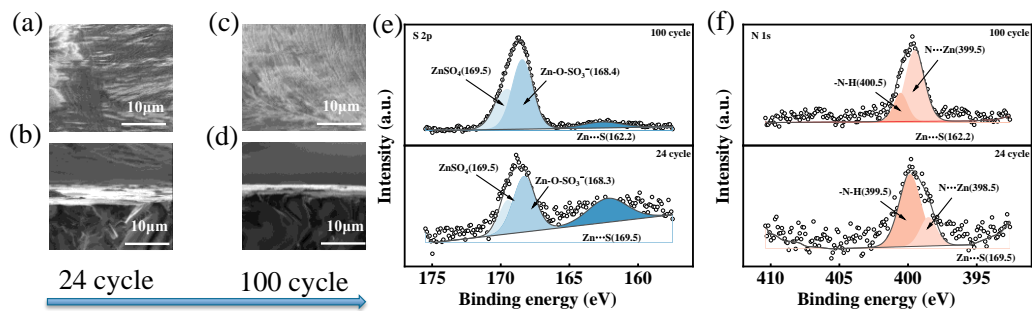


Figure S12. (a)~(d) Surface and cross-sectional and SEM images of the Zn anode cycled in the electrolyte with and without AMPS. (e) S 2p and (f) N 1s on Zn electrode separated from electrolytes after 24/100 cycles with 1 mA cm^{-2} , 1 mAh cm^{-2} .

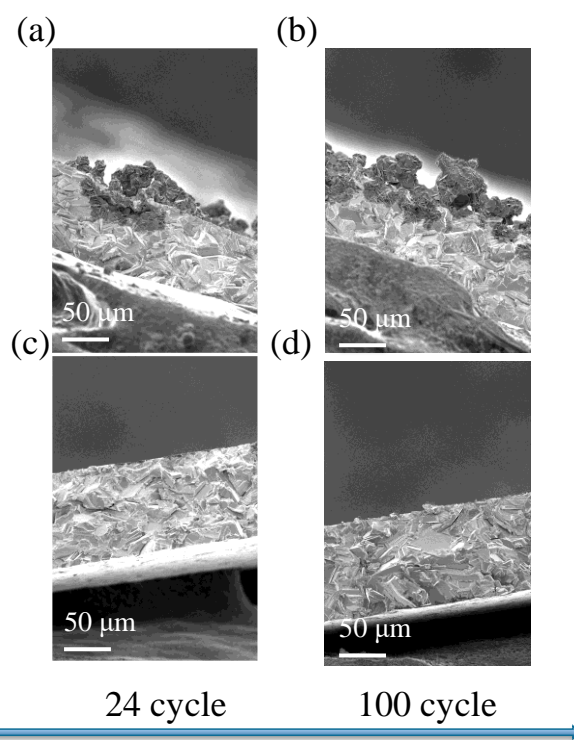


Figure S13. Cross-sectional SEM images of the interface of electrolyte/Zn anode in the electrolyte (a)~(b) without and (c)~(d) with AMPS.

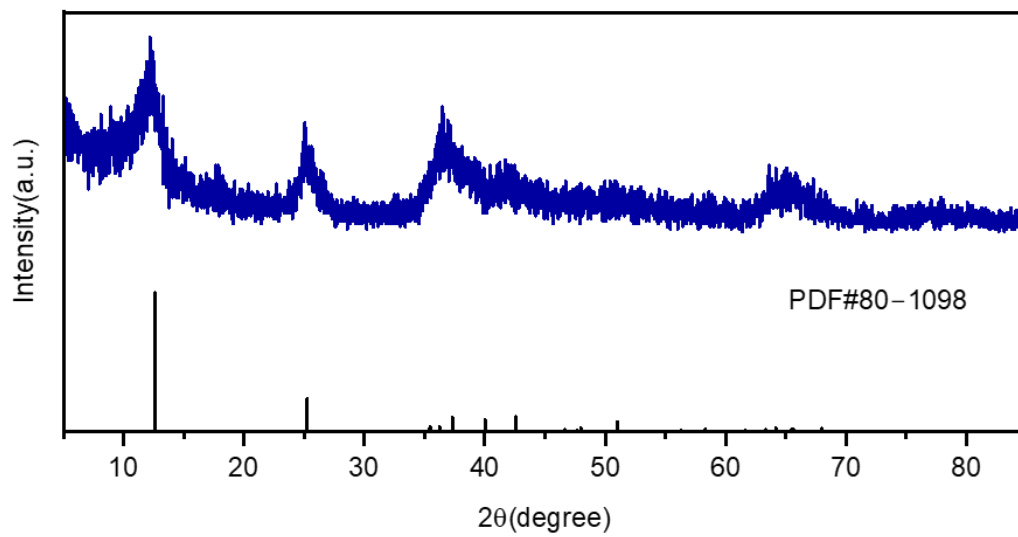


Figure S14. XRD pattern of MnO₂ cathode.

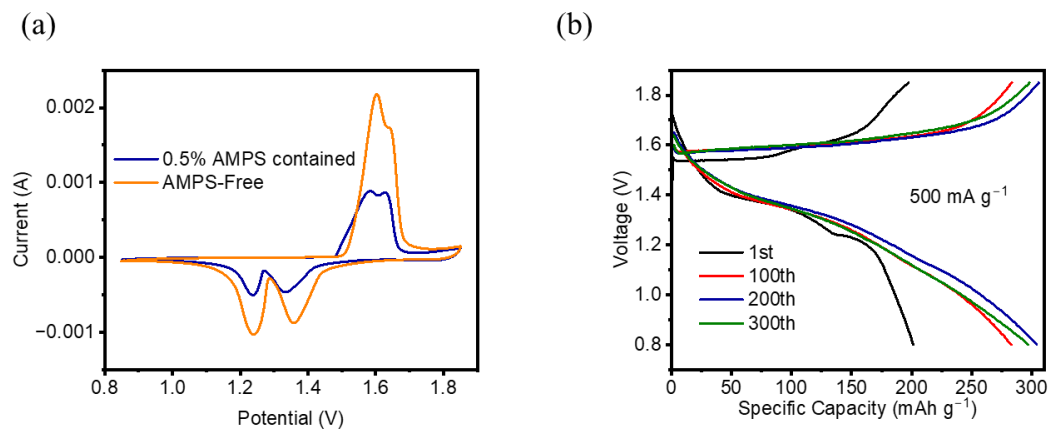


Figure S15. a) Cyclic voltammety curves of Zn||MnO₂ full cell with different electrolytes. b) Galvanostatic charge and discharge profiles of Zn||MnO₂ full cell with AMPS-added electrolyte.

Table S1 Comparison of the full cell's gravimetric energy density based on the cathode of literature-reported zinc battery systems.

Electrolytes	Cathodes	Energy density (Wh kg ⁻¹)	Cycle number	Ref.
1 M ZnSO₄+0.4 M MnSO₄	La ³⁺ - δ MnO ₂	375.9	200	13
2 M ZnSO₄+0.2 M MnSO₄	Cu ²⁺ - δ MnO ₂ Nanowire	497	700	14
2 M ZnSO₄+0.2 M MnSO₄	α -MnO ₂ /graphene Nanowire	406.6	3000	15
2 M ZnSO₄	Co ₃ O ₄ @- δ MnO ₂ /CC	212.8	250	16
1 M Zn(CF₃SO₃)₂+21 M LiTFSI	V ₂ O ₅	183	2000	17
2 M ZnSO₄	V ⁴⁺ -V ₂ O ₅	250	1000	18
-	NaV ₆ O ₁₅	337	150	19
3 M Zn(CF₃SO₃)₂	VO ₂	271.8	10000	20
Na₂SO₄+ZnSO₄	NiHCF	106	10000	21
ZHPE	ZHF	101	1000	22
This work	MnO₂	377	10000	

In Revision: Table R1 has been added into the revised SI.

References:

1. H. Huang, D. Xie, J. Zhao, P. Rao, W. M. Choi, K. Davey and J. Mao, *Adv. Energy Mater.*, 2022, 12, 2202419, DOI: 10.1002/aenm.202202419.
2. J. Cong, X. Shen, Z. Wen, X. Wang, L. Peng, J. Zeng and J. Zhao, *Energy Storage Mater.*, 2021, 35, 586–594, DOI: 10.1016/j.ensm.2020.11.041.
3. D. Han, Z. Wang, H. Lu, H. Li, C. Cui, Z. Zhang, R. Sun, C. Geng, Q. Liang, X. Guo, Y. Mo, X. Zhi, F. Kang, Z. Weng and Q. H. Yang, *Adv. Energy Mater.*, 2022, 12, 2102982, DOI: 10.1002/aenm.202102982.
4. J. L. Yang, J. Li, J. W. Zhao, K. Liu, P. Yang and H. J. Fan, *Adv. Mater.*, 2022, 34, 2202382, DOI: 10.1002/adma.202202382.
5. Y. Qin, P. Liu, Q. Zhang, Q. Wang, D. Sun, Y. Tang, Y. Ren and H. Wang, *Small*, 2020, 16, 2003106, DOI: 10.1002/sml.202003106.
6. J. Liu, W. Song, Y. Wang, S. Wang, T. Zhang, Y. Cao, S. Zhang, C. Xu, Y. Shi, J. Niu and F. Wang, *J. Mater. Chem. A*, 2022, 10, 19218–19227, DOI: 10.1039/D2TA05528G.
7. W. Zhou, M. Chen, Q. Tian, J. Chen, X. Xu and C.-P. Wong, *Energy Storage Mater.*, 2022, 44, 57–65, DOI: 10.1016/j.ensm.2021.10.002.
8. L. Zhang, B. Zhang, T. Zhang, T. Li, T. Shi, W. Li, T. Shen, X. Huang, J. Xu, X. Zhang, Z. Wang and Y. Hou, *Adv. Funct. Mater.*, 2021, 31, 210186, DOI: 10.1002/adfm.202100186.
9. Y. Dong, L. Miao, G. Ma, S. Di, Y. Wang, L. Wang, J. Xu and N. Zhang, *Chem. Sci.*, 2021, 12, 5843–5852, DOI: 10.1039/D0SC06734B.
10. H. Liu, J.-G. Wang, Z. You, C. Wei, F. Kang and B. Wei, *Mater. Today*, 2021, 42, 73–98, DOI: 10.1016/j.mattod.2020.08.021.
11. S. Lian, C. Sun, W. Xu, W. Huo, Y. Luo, K. Zhao, G. Yao, W. Xu, Y. Zhang, Z. Li, K. Yu, H. Zhao, H. Cheng, J. Zhang and L. Mai, *Nano Energy*, 2019, 62, 79–84, DOI: 10.1016/j.nanoen.2019.04.038.
12. K. Zhao, C. Wang, Y. Yu, M. Yan, Q. Wei, P. He, Y. Dong, Z. Zhang, X. Wang and L. Mai, *Adv. Mater. Interfaces*, 2018, 5, 1800848, DOI: 10.1002/admi.201800848.
13. H. Zhang, Q. Liu, J. Wang, K. Chen, D. Xue, J. Liu and X. Lu, *J. Mater. Chem. A*, 2019, 7, 22079–22083.
14. R. Zhang, P. Liang, H. Yang, H. Min, M. Niu, S. Jin, Y. Jiang, Z. Pan, J. Yan, X. Shen and J. Wang, *Chem. Eng. J.*, 2022, **433**, 133687.
15. B. Wu, G. Zhang, M. Yan, T. Xiong, P. He, L. He, X. Xu and L. Mai, *Small*, 2018, **14**, 1703850.
16. N. Wang, G. Yang, Y. Gan, H. Wan, X. Chen, C. Wang, Q. Tan, J. Ji, X. Zhao, P. Liu, J. Zhang, X. Peng, H. Wang, Y. Wang, G. Ma, P. A. van Aken and H. Wang, *Front. Chem.*, DOI:10.3389/fchem.2020.00793.
17. P. Hu, M. Yan, T. Zhu, X. Wang, X. Wei, J. Li, L. Zhou, Z. Li, L. Chen and L. Mai, *ACS Appl. Mater. Interfaces*, 2017, **9**, 42717–42722.
18. F. Liu, Z. Chen, G. Fang, Z. Wang, Y. Cai, B. Tang, J. Zhou and S. Liang, *Nano-Micro Lett.*, 2019, **11**, 25.
19. S. Islam, M. H. Alfaruqi, B. Sambandam, D. Y. Putro, S. Kim, J. Jo, S. Kim, V. Mathew and J. Kim, *Chem. Commun.*, 2019, **55**, 3793–3796.

20. T. Wei, Q. Li, G. Yang and C. Wang, *J. Mater. Chem. A*, 2018, **6**, 8006–8012.
21. F. Ma, X. Yuan, T. Xu, S. Zhou, X. Xiong, Q. Zhou, N. Yu, J. Ye, Y. Wu and T. van Ree, *Energy Fuels*, 2020, **34**, 13104–13110.
22. S. Dilwale, P. P. Puthiyaveetil, A. Babu and S. Kurungot, *Small*, 2024, **20**, 2311923.